

DTP/97/24
DESY-97-084
May 1997
Revised August 1997

Radiative Corrections to the Photon + 1 Jet Rate at LEP

A. Gehrmann–De Ridder^a, T. Gehrmann^b and E. W. N. Glover^a

^a *Department of Physics, University of Durham, Durham DH1 3LE, England*

^b *DESY, Theory Group, D-22603 Hamburg, Germany*

Abstract

We present the results of a calculation of the rate for the annihilation of an e^+e^- pair into a jet containing an energetic photon and a single further jet at order $\alpha\alpha_s$. By comparing these results with the existing data on the photon + 1 jet rate from the ALEPH Collaboration, we make a first determination of the process independent quark-to-photon fragmentation function $D_{q\rightarrow\gamma}(z, \mu_F)$ at order $\alpha\alpha_s$. We also compare our prediction for the inclusive photon energy spectrum with the recent OPAL measurement.

The production of final state photons at large transverse momenta is one of the key observables studied in hadronic collisions. Data on high- p_T photon production yield valuable information on the gluon distribution in the proton. Moreover, if the Standard Model Higgs boson has a mass lying below the WW -threshold, one of the best detection channels at the CERN LHC is via its two photons decay mode [1]. A precise understanding of the background processes yielding two photon final states is therefore crucial for Higgs searches at the LHC.

Photons produced in hadronic collisions arise essentially from two different sources: ‘direct’ or ‘prompt’ photon production via the hard partonic processes such as $qg \rightarrow q\gamma$ and $q\bar{q} \rightarrow g\gamma$ or through the ‘fragmentation’ of a hadronic jet into a single photon carrying a large fraction of the jet energy. The former gives rise to perturbatively calculable short-distance contributions whereas the latter is primarily a long distance process which cannot be calculated perturbatively and is described in terms of the quark-to-photon fragmentation function [2]. In principle, this fragmentation contribution could be suppressed to a certain extent by imposing isolation cuts on the photon, typically formulated by limiting the amount of hadronic energy allowed within an isolation cone around the photon. However, the matching of experimental isolation cones onto a theoretical calculation beyond the lowest order level is far from trivial [3, 4], and it has been shown that a sizeable contribution to the isolated photon cross section from the quark-to-photon fragmentation process remains even after isolation cuts have been applied [5].

All estimates of the fragmentation contribution to the production of one or two final state photons in hadron collisions so far [6] have had to rely on a model of the photon fragmentation function. This function obeys a perturbative evolution equation with a non-perturbative boundary condition usually parameterized in the form of an initial distribution at some low starting scale μ_0 . Several models, based either on an asymptotic solution of the evolution equation [7] or on estimates of the non-perturbative boundary conditions inspired by Vector Meson Dominance models [8] can be found in the literature. It is clear that the lack of a precise knowledge on the quark-to-photon fragmentation function introduces a *non-quantifiable* systematic uncertainty into any theoretical calculation of photon production cross sections. A precise determination of the process independent quark-to-photon fragmentation function is therefore needed and the results obtained in the remainder of this letter should help to achieve this.

A first measurement of the quark-to-photon fragmentation function has been performed [9] by the ALEPH collaboration at CERN from an analysis of two jet events in which one of the jets contains a photon carrying a large fraction ($z > 0.7$) of the jet energy. In these ‘photon’ + 1 jet events, a democratic approach is used to group the particles into jets and the photon is clustered simultaneously with the other hadrons. A comparison between this measured rate and the calculated rate up to $\mathcal{O}(\alpha)$ [10] yielded a first determination [9] of the quark-to-photon fragmentation function accurate at this order. Both theoretical and experimental analyses used the Durham jet algorithm [11]. Note that z , the fraction of electromagnetic energy within the ‘photon’ jet, is in general different from the parameter x_γ considered in inclusive photon production [12]. In the collinear core of the ‘photon jet’ however, where the non-perturbative effects arise, the definitions of these two parameters coincide.

In the present letter, we report the results of a calculation of the $\mathcal{O}(\alpha\alpha_s)$ QCD corrections to the ‘photon’ + 1 jet rate, performed using the same democratic approach. Together with the published data [9], this enables us to obtain a first determination of the process independent quark-to-photon fragmentation function at $\mathcal{O}(\alpha\alpha_s)$. The details of this calculation will be presented in a subsequent publication [13].

A common feature of all model estimates of the quark-to-photon fragmentation function [7, 8] is the resummation of leading ($\alpha_s^n \log^{n+1} \mu_F^2$) and subleading ($\alpha_s^n \log^n \mu_F^2$) logarithms of the mass factorization scale μ_F to all orders in the strong coupling constant. The results of this resummation procedure seem to suggest that the photon fragmentation function is $\mathcal{O}(\alpha/\alpha_s)$ and that quark and gluon fragmentation into photons contribute at the same order. This view is widely held for the photon fragmentation as well as for the photon structure function. However, in the region of high z and where jets are resolved, this is not necessarily the correct procedure to adopt. For example, the distribution of electromagnetic energy within the photon jet of photon + 1 jet events, for a single quark of charge e_q , can be written [10],

$$\frac{1}{\sigma_0} \frac{d\sigma}{dz} = 2D_{q\rightarrow\gamma}(z, \mu_F) + \frac{\alpha e_q^2}{\pi} P_{q\gamma}^{(0)}(z) \log\left(\frac{s_{\text{cut}}}{\mu_F^2}\right) + \dots, \quad (1)$$

where \dots represents terms where the photon is perturbatively isolated (proportional to $\delta(1-z)$) and other perturbative contributions which are well behaved as $z \rightarrow 1$. The non-perturbative fragmentation function is a solution of,

$$\frac{\partial D_{q\rightarrow\gamma}}{\partial \log \mu_F^2} = \frac{\alpha e_q^2}{2\pi} P_{q\gamma}^{(0)}(z) + \dots, \quad (2)$$

and s_{cut} is determined by the jet clustering algorithm. In the Durham jet clustering algorithm and at large z , $s_{\text{cut}} \sim sz(1-z)^2/(1+z) \sim p_T^2$ [10] where p_T is the transverse momentum of the photon with respect to the cluster. In the usual approach, the solution of the evolution equation for $D_{q\rightarrow\gamma}$, is proportional to $\log(\mu_F^2/\mu_0^2)$ where μ_0 is some small scale and the conventional assignment of a power of $1/\alpha_s$ to the fragmentation function is clearly motivated. For ‘physical’ scale choices, $\mu_F^2 \sim s_{\text{cut}}$,¹ and the perturbative contribution is suppressed relative to the fragmentation contribution, so that for $z < 1$, the fragmentation function is indeed more significant. However, at large z , we see that the transverse size of the photon jet cluster decreases such that $s_{\text{cut}} \rightarrow 0$. The hierarchy $s_{\text{cut}} \sim \mu_F^2$ and $\mu_F^2 \gg \mu_0^2$ is no longer preserved and both contributions in eq. (1) are important. Large logarithms of $(1-z)$ are the most dominant contributions. Since, from the experimental point of view, we are required to observe isolated or almost isolated photons, this is precisely the region that we are most interested in. For this reason, we choose not to impose the conventional prejudice and resum the logarithms of μ_F *a priori*. Instead, we work within a fixed order framework, to isolate the relevant large logarithms.

As mentioned above, potentially large logarithms of $(1-z)$ are present and need to be resummed. At present however, we have not accomplished this resummation and, to avoid

¹For inclusive processes, $s_{\text{cut}} \sim s$ is more appropriate.

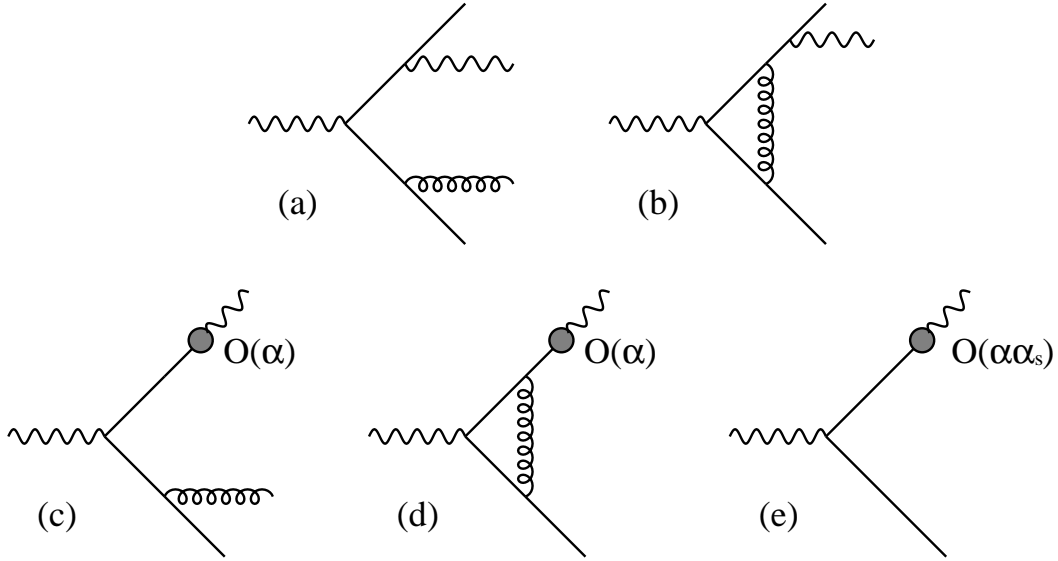


Figure 1: Parton level subprocesses contributing to the photon + 1 jet rate at $\mathcal{O}(\alpha\alpha_s)$.

unstable behaviour at large z , we choose a form of the fragmentation function that renders the calculation well behaved as $z \rightarrow 1$. This approach is identical to the procedure applied in the lowest order calculation [10] and in the lowest order experimental analysis [9]. It is thus possible to make a direct comparison of our next-to-leading order results with these earlier leading order results, and to test the stability of the perturbative fixed order approach.

The photon + 1 jet rate in e^+e^- annihilation at $\mathcal{O}(\alpha\alpha_s)$ receives contributions from five parton-level subprocesses displayed in Fig. 1:

- (a) The tree level process $\gamma^* \rightarrow q\bar{q}g\gamma$, where the final state particles are clustered together such that a ‘‘photon jet’’ and one additional jet are observed in the final state.
- (b) The one loop gluon correction to the $\gamma^* \rightarrow q\bar{q}\gamma$ process, where the photon and one of the quarks are clustered together or the photon is isolated while both quarks form a single jet.
- (c) The process $\gamma^* \rightarrow q\bar{q}g$, where one of the quarks fragments into a photon while the remaining partons form only a single jet.
- (d) The one loop gluon correction to the $\gamma^* \rightarrow q\bar{q}$ process, where one of the quarks fragments into a photon.
- (e) The tree level process $\gamma^* \rightarrow q\bar{q}$ with a generic $\mathcal{O}(\alpha\alpha_s)$ counterterm present in the *bare* quark-to-photon fragmentation function.

Although the ‘photon’ + 1 jet cross section is finite at $\mathcal{O}(\alpha\alpha_s)$, all these contributions contain divergences (when the photon and/or the gluon are collinear with one of the quarks,

when the gluon is soft or because the bare quark-to-photon fragmentation function contains infinite counter terms). These divergences need to be isolated and cancelled analytically. It is only after this cancellation has taken place, that it is possible to numerically evaluate the remaining finite contributions in a Monte Carlo program containing the experimental jet reconstruction algorithm, and ultimately to evaluate the ‘photon’ + 1 jet rate at $\mathcal{O}(\alpha\alpha_s)$.

The assignment of a single power of α to the quark-to-photon fragmentation function (and $\mathcal{O}(\alpha\alpha_s)$ to the gluon-to-photon fragmentation function) carries through when factorizing the explicit singularities present in the real and virtual processes with photon emission into the fragmentation functions. Here, the leading perturbative counterterm in the quark-to-photon fragmentation function is $\mathcal{O}(\alpha)$ while the leading counterterm in the gluon-to-photon fragmentation function is $\mathcal{O}(\alpha\alpha_s)$. Consequently, the gluon-to-photon fragmentation function plays no role at the fixed order $\mathcal{O}(\alpha\alpha_s)$; since radiating the gluon contributes an additional factor of α_s , it first contributes at $\mathcal{O}(\alpha\alpha_s^2)$. In fact, all of the model estimates [7, 8] indicate that the gluon-to-photon fragmentation is orders of magnitude smaller than the quark-to-photon fragmentation function at large z and we ignore it throughout.

Following the philosophy of [14], we use the concept of a theoretical resolution criterion s_{\min} to define the singular regions. Within the singular regions, the matrix elements are approximated and the unresolved variables analytically integrated. At next-to-leading order, most QCD processes receive singular contributions when either one gluon is soft or two particles are collinear – in other words a single particle is theoretically unresolved. However, the evaluation of the singular contributions associated with the process $\gamma^* \rightarrow q\bar{q}g\gamma$ is of particular interest as it contains various ingredients which could directly be applied to the calculation of jet observables at next-to-next-to-leading order. For example, there are contributions where *two* of the final state partons are theoretically unresolved. The three different double unresolved contributions which occur in this calculation are: the *triple collinear* contributions, arising when the photon and the gluon are simultaneously collinear to one of the quarks, the *soft/collinear* contributions arising when the photon is collinear to one of the quarks while the gluon is soft and the *double single collinear* contributions, resulting when the photon is collinear to one of the quarks while the gluon is collinear to the other. In addition, there are also single unresolved contributions from the one-loop $\gamma^* \rightarrow q\bar{q}\gamma$ process and from the tree-level fragmentation process $\gamma^* \rightarrow q\bar{q}g$ when two of the final state particles are collinear. A detailed derivation of each of these singular contributions, along with how the different single and double unresolved regions match onto each other, will be presented in [13].

The combination of the unresolved contributions present in the processes shown in Fig. 1(a)-(d) yields a result that still contains single and double poles in ϵ . These pole terms however are proportional to the universal next-to-leading order splitting function $P_{q\gamma}^{(1)}$ [15] and a convolution of two lowest order splitting functions, $(P_{qq}^{(0)} \otimes P_{q\gamma}^{(0)})$. Hence, they are factorized into the next-to-leading order counterterm of the bare quark-to-photon fragmentation function [16] present in the contribution depicted in Fig. 1(e), yielding a finite and factorization scale (μ_F) dependent result [13].

Once the singularities have been removed, the remaining finite contributions can be

numerically evaluated. Often this is realized within the *phase space slicing* method, first introduced by [17] and further developed in [14] for general next-to-leading order QCD processes. The original formulation of the phase space slicing method requires the analytical calculation of an approximated matrix element inside the theoretically unresolved regions, while the full matrix element is evaluated numerically only outside any singular region. This procedure turns out to be inappropriate where more than one particle is potentially unresolved. Apart from generically double unresolved regions, we find areas in the four parton phase space which belong simultaneously to two different single unresolved regions. Those areas are not treated correctly within the phase space slicing procedure. A consistent treatment is possible in the *hybrid subtraction* method developed in [18]. This scheme attempts to combine the advantages of the phase space slicing procedure with the alternative *subtraction* methods [19]. The parton resolution parameter is used to isolate the poles, but, rather than assuming that the approximated matrix elements are exact, the difference between the full matrix element and its approximation is numerically evaluated in all unresolved regions.

The numerical program finally evaluating the ‘photon’ + 1 jet rate at $\mathcal{O}(\alpha\alpha_s)$ contains four separate contributions. These contributions are determined according to the number of partons in the final state and the presence or absence of the quark-to-photon fragmentation function. For each final state, ‘photon’ + 1 jet events are selected using a democratic jet clustering algorithm and a given value of the jet resolution parameter y_{cut} . The “fragmentation function” used in the numerical evaluation of the cross section is the sum of the μ_F -dependent quark-to-photon fragmentation function and a finite contribution from the unresolved photon region. The four contributions are:

(A) **2 partons + photon**

This contribution corresponds to the process $\gamma^* \rightarrow q\bar{q}\gamma$ with a hard photon in the final state. It is present at $\mathcal{O}(\alpha)$ and $\mathcal{O}(\alpha\alpha_s)$ (due to the presence of a theoretically unresolved real or virtual gluon).

(B) **2 partons + “fragmentation”**

The $\gamma^* \rightarrow q\bar{q} \otimes D_{q \rightarrow \gamma}$ process is present at $\mathcal{O}(\alpha)$ and $\mathcal{O}(\alpha\alpha_s)$. In particular, it contains the finite terms corresponding to the $q - \gamma$ collinear region at $\mathcal{O}(\alpha)$ and the finite parts associated with all double unresolved regions at $\mathcal{O}(\alpha\alpha_s)$.

(C) **3 partons + photon**

This contribution is only present at $\mathcal{O}(\alpha\alpha_s)$ and describes the $\gamma^* \rightarrow q\bar{q}\gamma g$ process where both photon and gluon are theoretically resolved.

(D) **3 partons + “fragmentation”**

The $\gamma^* \rightarrow q\bar{q}g \otimes D_{q \rightarrow \gamma}$ process with a hard gluon in the final state, is only present at $\mathcal{O}(\alpha\alpha_s)$.

Each of the contributions listed above depends logarithmically (in fact as $\log^3(y_{\text{min}})$) on the theoretical resolution parameter $y_{\text{min}} = s_{\text{min}}/Q^2$, which is used throughout the calculation to divide the final state phase space into different resolved and unresolved regions. However, the physical ‘photon’ + 1 jet cross section, which is the sum of all theoretically resolved and

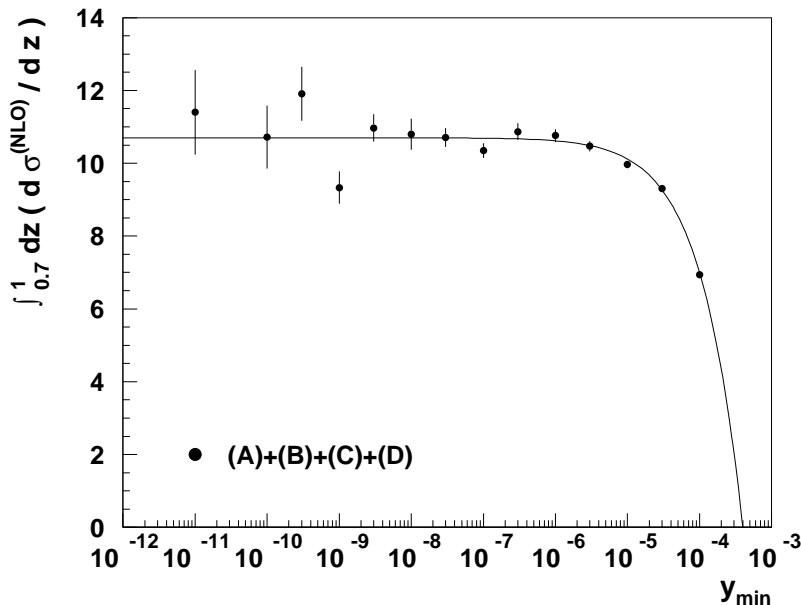


Figure 2: Sum of all $\mathcal{O}(\alpha_s)$ contributions to the total photon + 1 jet rate for a single quark of charge e_q such that $\alpha e_q^2 = 2\pi$, $\alpha_s(N^2 - 1)/2N = 2\pi$ using the Durham jet algorithm with $y_{\text{cut}} = 0.1$, and integrated for $z > 0.7$.

unresolved contributions, *must* of course be independent of the choice of y_{\min} . That this is indeed the case is illustrated in Fig. 2 where we show the sum of all $\mathcal{O}(\alpha_s)$ contributions to the total rate as a function of y_{\min} . For simplicity, we show only the $\mathcal{O}(\alpha_s)$ contribution for a single quark of charge e_q such that $\alpha e_q^2 = 2\pi$, $\alpha_s(N^2 - 1)/2N = 2\pi$ using the Durham jet algorithm with $y_{\text{cut}} = 0.1$, and integrated for $z > 0.7$. We see that the cross section approaches (within numerical errors) a constant value provided that y_{\min} is chosen to be small enough, indicating a complete cancellation of all powers of $\log(y_{\min})$. This provides a strong check on the correctness of our results and on the consistency of our approach. The behavior at large values of y_{\min} can be understood to be due to terms proportional to $y_{\min} \log^2(y_{\min})$, which have been neglected in the analytic evaluation of all theoretically unresolved contributions. It can clearly be seen that these terms are already unimportant at $y_{\min} = 10^{-6}$, which will be used in all numerical studies below.

We can now determine the quark-to-photon fragmentation function $D(z, \mu_F)$ up to this order from a comparison between the measured ‘photon’ + 1 jet rate [9] and the results of our calculation. This function, which parameterizes the perturbatively incalculable long-distance contribution to the photon radiation off a quark has to satisfy a perturbative evolution equation in the factorization scale μ_F . All unknown long-distance contributions can therefore be attributed to the behavior of $D(z, \mu_0)$, the initial value of this fragmentation function, which is to be fitted to the experimental data, at some low scale μ_0 . Indeed, the next-to-leading order fragmentation function can be expressed as an *exact* solution of the evolution

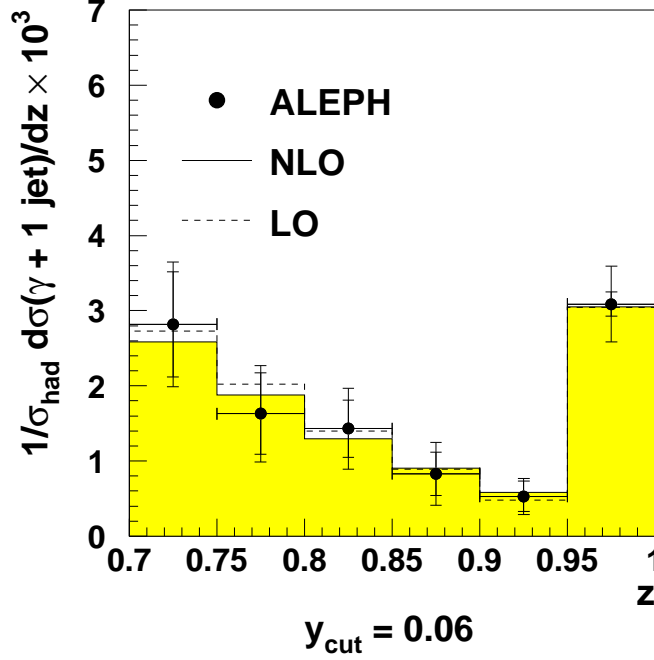


Figure 3: Comparison of the ‘photon’ + 1 jet rate at $\mathcal{O}(\alpha)$ and $\mathcal{O}(\alpha\alpha_s)$ with the ALEPH data ($y_{\text{cut}} = 0.06$), including the fitted quark-to-photon fragmentation function.

equation up to $\mathcal{O}(\alpha\alpha_s)$ [13],

$$\begin{aligned}
D(z, \mu_F) = & D(z, \mu_0) + \frac{\alpha e_q^2}{2\pi} P_{q\gamma}^{(0)}(z) \log\left(\frac{\mu_F^2}{\mu_0^2}\right) + \frac{\alpha e_q^2 \alpha_s}{2\pi} \left(\frac{N^2 - 1}{2N}\right) P_{q\gamma}^{(1)}(z) \log\left(\frac{\mu_F^2}{\mu_0^2}\right) \\
& + \frac{\alpha_s}{2\pi} \left(\frac{N^2 - 1}{2N}\right) \log\left(\frac{\mu_F^2}{\mu_0^2}\right) P_{qq}^{(0)}(z) \otimes \left[\frac{\alpha e_q^2}{2\pi} \frac{1}{2} P_{q\gamma}^{(0)}(z) \log\left(\frac{\mu_F^2}{\mu_0^2}\right) + D(z, \mu_0) \right].
\end{aligned} \tag{3}$$

It should be re-emphasized that this solution does not take the commonly implemented (e.g. [7, 8]) resummations of $\log \mu_F^2$ into account. As explained above, this appears the only consistent procedure since powers of $\log(1 - z)$ may be of equal importance in the large z region [20], which is the main region of interest in the present study. Finally, this procedure is identical to the procedure applied in earlier theoretical [10] and experimental [9] analyses at lowest order, such that a direct and self-consistent quantification of the next-to-leading order effects in the ‘photon’ + 1 jet rate becomes feasible.

Furthermore, since this solution is exact at the order under consideration, the factorization scale dependence of the ‘photon’ + 1 jet rate is eliminated, i.e. our results are independent of the choice of μ_F .

A three parameter fit to the ALEPH ‘photon’ + 1 jet data [9] for the z distribution,

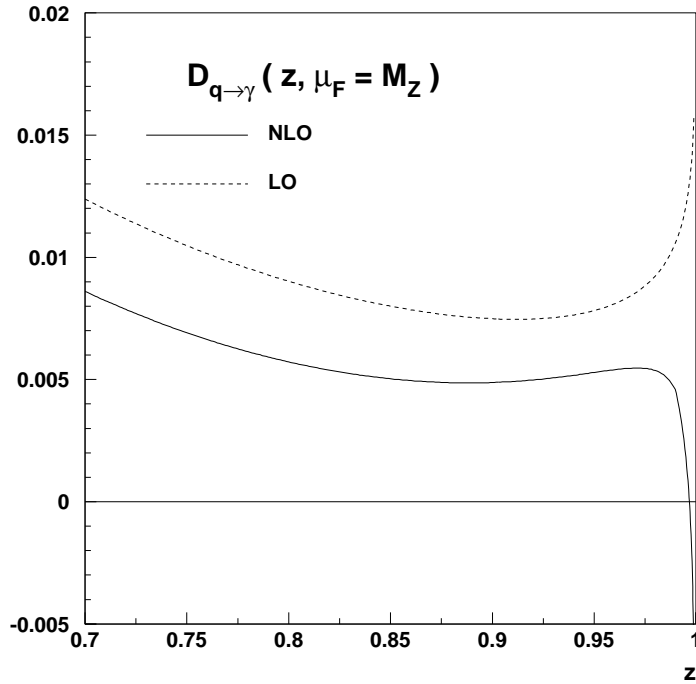


Figure 4: The measured quark-to-photon fragmentation function at leading [9] and next-to-leading (this study) order for a quark of unit charge. The factorization scale is taken to be $\mu_F = M_Z$.

$\frac{1}{\sigma_0} \frac{d\sigma}{dz}$, for the jet resolution parameter $y_{\text{cut}} = 0.06$ and $\alpha_s(M_Z^2) = 0.124^2$ yields,

$$D^{NLO}(z, \mu_0) = \frac{\alpha e_q^2}{2\pi} \left(-P_{q\gamma}^{(0)}(z) \log(1-z)^2 + 20.8(1-z) - 11.07 \right), \quad (4)$$

where $\mu_0 = 0.64$ GeV. For reference, the lowest order fit obtained by the ALEPH Collaboration [9] is,

$$D^{LO}(z, \mu_0) = \frac{\alpha e_q^2}{2\pi} \left(-P_{q\gamma}^{(0)}(z) \log(1-z)^2 - 13.26 \right), \quad (5)$$

with $\mu_0 = 0.14$ GeV. In both cases, the logarithmic term proportional to $P_{q\gamma}^{(0)}(z)$ is introduced to ensure that the predicted z distribution is well behaved as $z \rightarrow 1$ [10]. It should be kept in mind that both parameterizations are only fitted to data with $z > 0.7$, which is thus the natural limit of their validity.

The ALEPH data and the results of the $\mathcal{O}(\alpha_s)$ calculation using the fitted next-to-leading order fragmentation function are shown in Fig. 3. (For reference, we have also displayed the $\mathcal{O}(\alpha)$ prediction [10] using the ALEPH fit of the lowest order fragmentation function [9].) The fit also provides a good description of the z distribution for other values of y_{cut} [13]. This is to be expected since the non-perturbative effects are largely in the

²At this order, all choices of the strong coupling constant are equally valid. This value of α_s is chosen so that the observed hadronic cross section is reproduced by the $\mathcal{O}(\alpha_s)$ calculation.

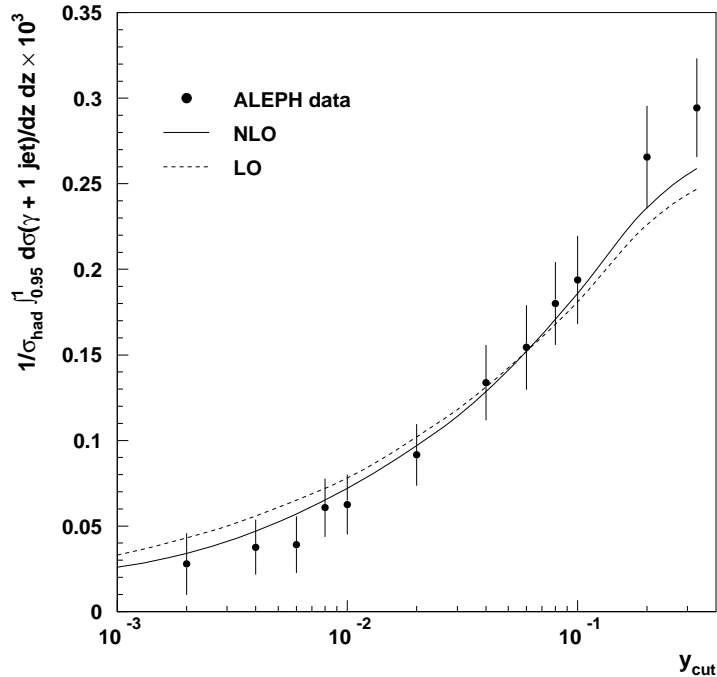


Figure 5: The integrated photon + 1 jet rate above $z = 0.95$ as function of y_{cut} , compared with the $\mathcal{O}(\alpha)$ and $\mathcal{O}(\alpha\alpha_s)$ order calculations including the appropriate quark-to-photon fragmentation functions.

collinear core of the ‘photon’ jet which is fully contained within the jet definition. Moreover, it turns out that the next-to-leading order corrections are moderate for all values of y_{cut} , which clearly demonstrates the perturbative stability of our fixed order approach.

The resulting next-to-leading order ($\overline{\text{MS}}$) quark-to-photon fragmentation function (for a quark of unit charge) at a factorization scale $\mu_F = M_Z$ is shown in Fig. 4 and compared with the lowest order fragmentation function obtained in [9]. A large difference between the leading and next-to-leading order quark-to-photon fragmentation functions is observed only for z close to 1, indicating the presence of large $\log(1 - z)$.

Having described the z distribution in the measured range, we shall now focus only on the ‘photon’ + 1 jet rate for $z > 0.95$ which can be viewed as the *isolated* photon + 1 jet rate in the democratic clustering approach [9]. This division between isolated and non-isolated is motivated both by the measured z distribution (see Fig. 3) and the observation that hadronization effects cause the photon jet to have a z value slightly less than unity [9]. In previous theoretical [12, 21, 22] and experimental [23] analyses of isolated photon + n jet rates, the candidate photon was isolated from the other hadrons using a geometrical cone, *before* these hadrons were clustered into jets by the jet recombination algorithm. The photon was said to be ‘isolated’ if it was accompanied only by a small (but non-zero) amount of hadronic energy inside the cone. As a result of these analyses it was found that large negative next-to-leading order corrections were needed to obtain a reasonable agreement between

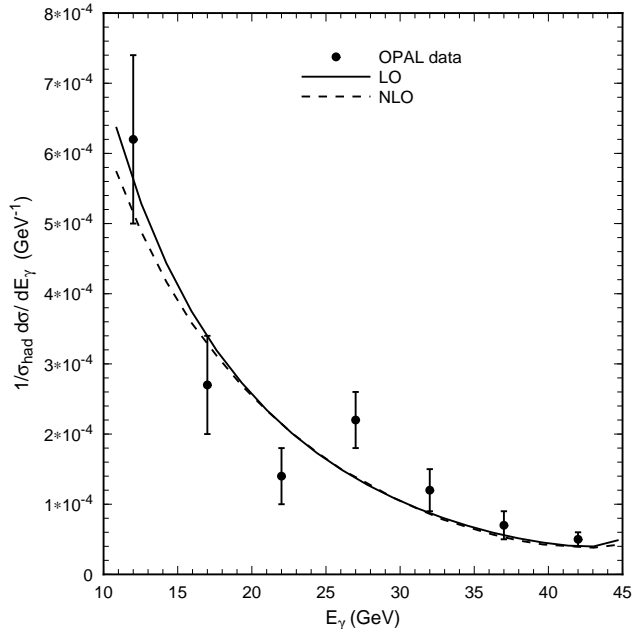


Figure 6: The inclusive photon energy distribution normalized to the hadronic cross section as measured by the OPAL Collaboration compared with the $\mathcal{O}(\alpha)$ and $\mathcal{O}(\alpha\alpha_s)$ order calculations including the appropriate quark-to-photon fragmentation functions determined using the ALEPH photon + 1 jet data.

theory and experiment [21, 24]. Interestingly, a lowest order calculation of the photon + 1 jet rate for the cone algorithm using the process independent photon fragmentation function measured by ALEPH [9] and a suitable choice of z to define the isolation yields good agreement with the data [3].

Using the results of our calculation and the fitted quark-to-photon fragmentation function, we have determined the isolated photon + 1 jet rate in the democratic approach up to $\mathcal{O}(\alpha\alpha_s)$. The result of this calculation compared with data from ALEPH [9] and the leading order calculation [10] is shown in Fig. 5. It can clearly be seen that inclusion of the next-to-leading order corrections improves the agreement between data and theory over the whole range of y_{cut} . It is also apparent that the next-to-leading order corrections to the isolated photon + 1 jet rate obtained in this democratic clustering approach are of reasonable size indicating a better perturbative stability of this *isolated* photon definition.

As a final illustration of the generality of our results, we turn to the inclusive photon distribution recently measured by the OPAL Collaboration [25]. Here, jets are not defined and, rather than the distribution of electromagnetic energy within the cluster, the energy distribution of the photon is considered. OPAL are able to identify photons with energies with as little as 10 GeV, and have compared their results with the model estimates of [7, 8]. They find reasonable agreement with factorization scales $\mu_F \sim M_Z$, although the data is too

poor to discriminate between the models. Fig. 6 shows our (scale independent) predictions for the inclusive photon energy distribution at both leading and next-to-leading order. We see good agreement with the data, even though the phase space relevant for the OPAL data far exceeds that used to determine the fragmentation functions from the ALEPH photon + 1 jet data.

In summary, we have presented the results of a complete calculation [13] of the ‘photon’ + 1 jet rate at $\mathcal{O}(\alpha\alpha_s)$. Although only next-to-leading order in perturbation theory, this calculation contains several ingredients appropriate to the calculation of jet observables at next-to-next-to-leading order. In particular, we needed to generalize the phase space slicing method of [17, 14] to more than one theoretically unresolved particle and have analytically calculated the following double unresolved configurations [13]: the triple collinear factor, the soft/collinear factor and the double single collinear factor. The ‘photon’ + 1 jet rate was then evaluated for a democratic clustering algorithm with a Monte Carlo program using the hybrid subtraction method of [18]. The results of our calculation, when compared to the data [9] on the ‘photon’ + 1 jet rate obtained by ALEPH, enabled a first determination of the process independent quark-to-photon fragmentation function at $\mathcal{O}(\alpha\alpha_s)$ in a fixed order approach. As a first application, we have used this function to calculate the ‘isolated’ photon + 1 jet rate in a democratic clustering approach at next-to-leading order. The inclusion of the QCD corrections improves the agreement between theoretical prediction and experimental data. Moreover, it was shown that these corrections are moderate, demonstrating the perturbative stability of this particular isolated photon definition. Finally, we have computed the inclusive photon energy distribution and found good agreement with the recent OPAL data.

Acknowledgements

One of us (A.G.) would like to thank the DESY Theory Group for their kind hospitality during the later stages of this work. A.G. also acknowledges the financial support of the University of Durham through a Research Studentship (Department of Physics).

References

- [1] See for example, P. Aurenche et al. and C. Seez et al., Proceedings of the “Large Hadron Collider Workshop”, Aachen 1990, CERN report 90-10, vol. 2, p.83 and p.474.
- [2] K. Koller, T.F. Walsh and P.M. Zerwas, Z. Phys. **C2** (1979) 197;
E. Laermann, T.F. Walsh, I. Schmitt and P.M. Zerwas, Nucl. Phys. **B207** (1982) 205.
- [3] E.W.N. Glover and A.G. Morgan, Phys. Lett. **B334** (1994) 208.
- [4] W.B. Kilgore and W.T. Giele, Phys. Rev. **D55** (1997) 7183.
- [5] M. Glück, L.E. Gordon, E. Reya and W. Vogelsang, Phys. Rev. Lett. **73** (1994) 388.

- [6] P. Aurenche et al., Z. Phys. **C56** (1992) 589, Nucl. Phys. **B399** (1993) 34;
H. Baer, J. Ohnemus and J.F. Owens, Phys. Rev. **D42** (1990) 61;
M. Glück et al., ref. [5];
L.E. Gordon, Nucl. Phys. **B501** (1997) 175, 197;
B. Bailey, J. Ohnemus and J.F. Owens, Phys. Rev. **D46** (1992) 2018;
C. Coriano and L.E. Gordon, Nucl. Phys. **B469** (1996) 202, Phys. Rev. **D54** (1996)
781.
- [7] J.F. Owens, Rev. Mod. Phys. **59** (1987) 465;
D.W. Duke and J.F. Owens, Phys. Rev. **D26** (1982) 1600.
- [8] M. Glück, E. Reya and A. Vogt, Phys. Rev. **D48** (1993) 116;
L. Bourhis, M. Fontannaz and J.Ph. Guillet, preprint LPTHE-ORSAY 96/103 (hep-
ph/9704447).
- [9] ALEPH collaboration: D. Buskulic et al., Z. Phys. **C69** (1996) 365.
- [10] E.W.N. Glover and A.G. Morgan, Z. Phys. **C62** (1994) 311.
- [11] Yu.L. Dokshitzer, Contribution to the Workshop on Jets at LEP and HERA, J. Phys. **G17** (1991) 1441.
- [12] Z. Kunszt and Z. Trócsányi, Nucl. Phys. **B394** (1993) 139.
- [13] A. Gehrmann–De Ridder and E.W.N. Glover, Durham preprint DTP/97/26 (hep-
ph/9707224).
- [14] W.T. Giele and E.W.N. Glover, Phys. Rev. **D46** (1992) 1980.
- [15] G. Curci, W. Furmanski and R. Petronzio, Nucl. Phys. **B175** (1980) 27;
W. Furmanski and R. Petronzio, Phys. Lett. **97B** (1980) 437.
- [16] G. Altarelli, R.K. Ellis, G. Martinelli and S.-Y. Pi, Nucl. Phys. **B160** (1979) 301;
P.J. Rijken and W.L. van Neerven, Nucl. Phys. **B487** (1997) 233.
- [17] K. Fabricius, I. Schmitt, G. Kramer and G. Schierholz, Z. Phys. **C11** (1981) 315.
- [18] E.W.N. Glover and M.R. Sutton, Phys. Lett. **B342** (1995) 375.
- [19] R.K. Ellis, D.A. Ross and A.E. Terrano, Nucl. Phys. **B178** (1981) 421;
S. Frixione, Z. Kunszt and A. Signer, Nucl. Phys. **B467** (1996) 399;
S. Catani and M.H. Seymour, Nucl. Phys. **B485** (1997) 291.
- [20] B.R. Webber, J.Phys. **G17** (1991) 1493.
- [21] E.W.N. Glover and W.J. Stirling, Phys. Lett. **B295** (1992) 128.
- [22] G. Kramer and H. Spiesberger, Proc. Workshop on “Photon Radiation from Quarks”,
Annecy 1991, CERN Yellow Report 92-04, p.26.

- [23] DELPHI Collaboration: P. Abreu et al., *Z. Phys.* **C53** (1992) 555;
OPAL Collaboration: P.D. Acton et al., *Z. Phys.* **C54** (1992) 193;
ALEPH Collaboration: D. Buskulic et al., *Z. Phys.* **C57** (1992) 17;
L3 Collaboration: O. Adriani et al., *Phys. Lett.* **B292** (1992) 472.
- [24] E.W.N. Glover and A.G. Morgan, *Phys. Lett.* **B324** (1994) 487.
- [25] OPAL Collaboration: K. Ackerstaff et al., CERN preprint CERN-PPE/97-086 (hep-ex/9708020).